

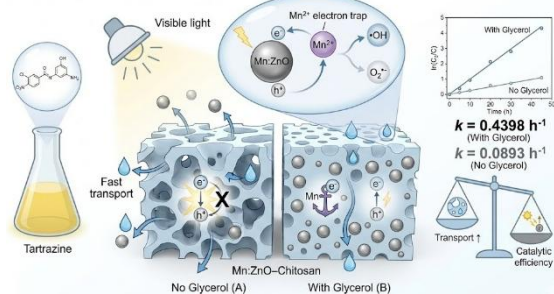
Effect of Glycerol Modification on Mn-Doped ZnO–Chitosan Membranes for Tartrazine Photodegradation

Nur Faridatus So'imah, Khabibi*, Retno Ariadi Lusiana

Department of Chemistry, Faculty of Science and Mathematics, Universitas Diponegoro, Semarang, Indonesia

ABSTRACT

This study evaluates the photocatalytic performance and charge transfer behavior of Mn-doped ZnO chitosan membranes, both with and without glycerol, for the degradation of tartrazine under visible light. The membranes were prepared by homogeneous mixing using chitosan as the polymer matrix, ZnO as the photocatalyst, Mn²⁺ as the dopant, and glycerol as a plasticizer. Membrane morphology and elemental distribution were examined using SEM and EDX, and supported by physical tests. Glycerol increased membrane flexibility and mechanical strength, but reduced porosity and surface hydrophilicity, indicating a denser polymer network and water accessibility. Photocatalytic activity was quantified from UV Vis monitoring of tartrazine and fitted to pseudo-first-order kinetics. The glycerol-containing membrane showed a higher rate constant ($k = 0.4398 \text{ h}^{-1}$) than the membrane without glycerol ($k = 0.0893 \text{ h}^{-1}$). The performance improvement is attributed to better catalyst retention and dispersion in the matrix, which supports photon utilization and charge separation. Mechanistic interpretation suggests that Mn²⁺ acts as an electron trap, thereby suppressing electron-hole recombination and promoting the formation of reactive species. At the same time, glycerol can suppress the generation of hydroxyl and superoxide radicals by limiting contact among tartrazine, water, and photocatalytically active sites. Overall, the results reveal a trade-off between transport properties and catalytic efficiency, identifying glycerol content as a key parameter for optimizing Mn-doped ZnO chitosan membranes for dye wastewater treatment.



Keywords: chitosan membrane; ZnO–doping Mn; glycerol; tartrazine photodegradation; charge transfer

*Corresponding Author: khabibi@live.undip.ac.id

How to cite: N.F. So'imah, Khabibi, and R.A. Lusiana, "Effect of Glycerol Modification on Mn-Doped ZnO–Chitosan Membranes for Tartrazine Photodegradation," *Jurnal Kimia dan Pendidikan Kimia (JKPK)*, vol. 10, no. 3, pp.506-526, 2025. [Online]. Available: <https://doi.org/10.20961/jkpk.v10i3.107512>

Received: 2025-08-02

Accepted: 2025-11-03

Published: 2025-12-31

INTRODUCTION

Increased industrial activity in the food and beverage sector has driven the widespread use of synthetic dyes, including tartrazine. Tartrazine is an azo dye, also known as Yellow E102 [1][2]. Azo dyes contain an $-\text{N}=\text{N}-$ group that produces intense color but is often resistant to degradation. Several azo dyes, including tartrazine, have been reported to exhibit carcinogenic and mutagenic effects, raising concerns regarding their safety in food

products and the environment [3]. Conventional treatment methods such as coagulation, adsorption, and filtration are often insufficient for complete dye removal [4][5]. Such processes primarily transfer pollutants from one phase to another rather than destroying the highly stable azo $-\text{N}=\text{N}-$ bond. Complete detoxification of tartrazine, therefore, generally requires oxidative degradation pathways [6]. An efficient and environmentally friendly treatment approach is therefore needed.

Photocatalysis is a promising option because it is a light-driven oxidation process that uses semiconductor materials to generate reactive radicals capable of decomposing complex organic contaminants [7][8]. Zinc oxide (ZnO) has attracted considerable attention as a photocatalyst due to its chemical stability, relatively low toxicity, and ability to generate reactive oxygen species for degrading persistent organic pollutants [9][10]. ZnO is widely used in photocatalysis due to its suitable band gap and high chemical stability [11]. However, pristine ZnO is primarily active under UV irradiation [12] and suffers from rapid electron-hole recombination, which limits its overall efficiency [13]. Electron-hole recombination reduces the availability of charge carriers required to produce key reactive species, such as hydroxyl radicals ($\cdot\text{OH}$) and superoxide radicals ($\text{O}_2\cdot^-$), which are essential for pollutant degradation [14]. One strategy to overcome these limitations is doping with transition metal ions such as Mn^{2+} , which can narrow the effective band gap and improve charge separation and charge transfer efficiency [15].

Mn^{2+} ions can function as electron and hole trapping sites, thereby promoting charge separation and improving photocatalytic activity. Incorporation of Mn into the ZnO lattice can narrow the effective band gap, enhance visible light absorption, and suppress electron-hole recombination by introducing additional energy levels within the band structure [16][17][18]. However, the direct use of Mn-doped ZnO powders is limited by difficulties in post-reaction separation and the potential risk of secondary

contamination [19]. A supporting matrix is therefore required to immobilize the photocatalyst, enabling more practical and scalable applications.

Chitosan, a natural biopolymer derived from chitin and commonly extracted from crustacean shells [20], is a promising candidate for this purpose. In comparison to other supports, such as cellulose, which often exhibits limited solubility [21][22], and synthetic polymers that may raise environmental concerns [23], chitosan offers a more sustainable and functional platform for photocatalyst immobilization [24]. Chitosan contains amino and hydroxyl groups that can interact strongly with metal oxide nanoparticles [25], and it can be readily processed into membrane forms. In addition to being biodegradable and environmentally benign, chitosan-based membranes offer favorable water permeability and mechanical integrity. The integration of Mn-doped ZnO into chitosan membranes, therefore, offers a solid-supported system for dye wastewater degradation that is easier to handle, control, and reuse [26].

Another challenge in developing photocatalytic membranes is maintaining membrane flexibility, ensuring homogeneous nanoparticle dispersion within the polymer matrix, and preserving mechanical integrity during photocatalytic operation. A commonly used strategy is the incorporation of plasticizers such as glycerol [27]. Glycerol can enhance the flexibility and improve the homogeneity of chitosan-based membranes through hydrogen bonding with the hydroxyl groups of chitosan [28][29]. Glycerol is often selected because it is highly polar, has a

strong affinity toward hydroxyl and amino groups in chitosan, and can reduce intermolecular interactions within the polymer network [30]. These effects increase chain mobility and improve membrane elasticity. Compared to higher molecular weight plasticizers such as polyethylene glycol, glycerol can diffuse more uniformly into the polymer matrix, allowing for more consistent modification [31]. Its renewable origin and low toxicity also support the development of environmentally friendly functional membranes [32].

Although ZnO and chitosan-based photocatalytic membranes have been widely reported, systematic comparisons of chitosan Mn-doped ZnO membranes with and without glycerol remain limited, particularly regarding degradation efficiency, charge transfer pathways, and reaction kinetics. Glycerol can also potentially inhibit interfacial charge transfer between the ZnO phase and the reaction medium when its concentration or interactions with other components are not optimized [33]. Strong hydrogen bonding between glycerol and surface hydroxyl groups on ZnO, combined with interactions with chitosan, may form a barrier layer around photocatalyst particles, reducing their direct contact with the solution. This condition can limit the migration of photogenerated charge carriers (e^- and h^+) and decrease the formation of reactive radicals, such as hydroxyl and superoxide ($\cdot OH$ and $O_2\cdot^-$), ultimately reducing photocatalytic degradation efficiency [33][34][35].

This study addresses this gap by directly comparing the photocatalytic performance, mechanistic pathways, and

kinetic behavior of chitosan-Mn-doped ZnO membranes with and without glycerol for the degradation of tartrazine. The influence of glycerol concentration on the photocatalytic performance of dye wastewater has not been systematically evaluated. Previous work has often treated glycerol primarily as a beneficial additive that improves membrane physical properties, while giving limited attention to the potential environmental implications of using glycerol at excessive levels. Relevant findings have been reported for other photocatalytic systems. Hoang et al. (2021) investigated the combination of TiO₂ and SiO₂ with glycerol for methyl orange degradation in continuous reactors under solar irradiation and reported improved degradation with increasing glycerol concentration. However, higher glycerol loading may also increase the organic burden in treated water. Follow-up studies in 2023 further suggested that excessive glycerol can negatively affect film performance by reducing reactive oxygen species formation and inhibiting dye degradation through interference with charge transfer efficiency at the polymer photocatalyst interface [33][34][36].

Accordingly, this study evaluates the role of glycerol in chitosan Mn-doped ZnO photocatalytic membranes by linking tartrazine degradation performance to membrane physicochemical properties and reaction kinetic parameters. The results are expected to provide quantitative evidence clarifying whether glycerol acts as a performance enhancer or instead suppresses photocatalytic efficiency. Such insight can support the design of biopolymer-

based photocatalytic membranes that are more effective, environmentally responsible, and suitable for practical water purification and green industrial applications.

METHODS

1. Materials and Tools

The chemicals used in this study include 30% Mn-doped ZnO. 30% Mn-doped ZnO is made of zinc acetate dihydrate ($\text{Zn}(\text{CH}_3\text{COO})_2 \cdot 2\text{H}_2\text{O}$) doped with manganese(II) acetate tetrahydrate ($\text{Mn}(\text{CH}_3\text{COO})_2 \cdot 4\text{H}_2\text{O}$). The 30% Mn doping refers to a weight percentage (wt%) relative to the total mass of Mn and ZnO, in the presence of NaOH 1N, chitosan, CH₃COOH, tartrazine, and aquadest.

This research utilizes a range of laboratory tools for the synthesis, characterization, and photocatalytic testing of materials. The main tools used include measuring cups, beaker glasses, a magnetic stirrer with a hotplate for mixing and heating solutions, and ovens for drying and calcining materials. In addition, centrifugators are used for precipitate separation, homogenizers for mixing chitosan solutions with ZnO nanoparticles, and petri dishes serve as a medium for forming circular-shaped membranes (diameter 90 mm). The pH of the solution is measured using a digital pH meter. Material characteristics analysis employs several primary instruments, including UV-Vis, SEM, Universal Testing Machine (UTM), and screw micrometers.

2. Manufacture of Chitosan-Mn-Doped ZnO Membrane Without Glycerol

2.5% chitosan is dissolved in 1% acetic acid solution. Mix until dissolved. Add 30%

Mn-doped ZnO to the Chitosan solution. Homogenize using a homogenizer for 6 hours at 4000 rpm [37]. The gel is poured into a membrane mold and cured at a temperature of 40-45 °C for 36 hours. The dry film is soaked for 24 hours in 1N NaOH at room temperature to facilitate detachment from the petri dish and to neutralize residual acetic acid from the chitosan dissolution. However, it can also trigger internal structural modifications, especially in chitosan-ZnO interactions. Residue is removed by rinsing the film with distilled water. After 8 hours of drying at 70 degrees Celsius, the membrane is stored in a desiccator before being used for photocatalytic degradation [20][29][37][38].

Dissolve 2.5% chitosan into 1% acetic acid solution. ZnO-dop Mn 30% is mixed for 30 minutes with glycerol to produce a ZnO-dop Mn 30%/glycerol solution. Glycerol was added as a plasticizer at a concentration of 1–6% (w/w) relative to the chitosan weight. Add the ZnO/glycerol solution to the chitosan solution. Homogenize using a homogenizer for 6 hours at 4000 rpm [37]. The gel is poured into a membrane mold and cured at a temperature of 40-45 °C for 36 hours. The dry film is soaked for 24 hours in 1N NaOH at room temperature to facilitate detachment from the petri dish and to neutralize residual acetic acid from the chitosan dissolution. However, it can also trigger internal structural modifications, especially in chitosan-ZnO interactions and glycerol stability in the matrix. Residue is removed by rinsing the film with distilled water. After 8 hours of drying at 70 degrees Celsius, the membrane is stored in a desiccant before being used for photocatalytic degradation [20][29][37][38].

3. Membrane Surface Morphology Analysis

Visualization of the membrane surface was carried out to determine the morphology and structure of the pores formed due to the addition or absence of glycerol. These visual characteristics are important for relating the physical and mechanical properties of the membrane to its structure. Micromorphological analysis of the membrane surface was performed using Scanning Electron Microscope-Energy Dispersive X-ray Spectroscopy (SEM-EDX) at acceleration voltages of 10 kV with magnifications of 1,000 \times , 5,000 \times , 10,000 \times , and 20,000 \times to determine the pore structure [39], the distribution of ZnO particles doping Mn in the chitosan matrix, and the effect of glycerol modification on the homogeneity of the membrane surface. Comparisons were made between membranes without glycerol and those with the addition of glycerol to observe differences in microstructure and the potential for nanoparticle agglomeration.

4. Membrane Physical Characterization

a. Membrane Thickness

Membrane thickness was measured using a digital micrometer at five different points for each sample, and the experiments were conducted in triplicate. The results are reported as the average value \pm standard deviation [40].

b. Tensile Strength

The tensile test is carried out using a Universal Testing Machine (UTM) [37]. The values of maximum tensile strength and elongation before breaking are used to compare the flexibility and mechanical

strength of glycerol-modified membranes with those that do not contain glycerol.

c. Porosity

The membrane is soaked in 10 mL of aqueduct for 24 hours. After that, the membrane is gently wiped and then weighed to determine its wet weight. Next, the membrane is dried and then weighed again to get its dry weight. The porosity test value can be calculated using the following formula:

$$\text{Porosity} = \frac{(w_1 - w_0)}{V \cdot \rho_w} \times 100\% \quad (1)$$

[37][41].

d. Water Contact Angle

The water contact angle test was performed to evaluate the surface roughness and wettability of the membranes using the sessile drop method with a droplet volume of 0.05 μ L. A contact angle of $<90^\circ$ indicates a hydrophilic surface, where water easily spreads and shows high affinity to the membrane, whereas a contact angle of $>90^\circ$ indicates a hydrophobic surface, where water forms spherical droplets with low interaction to the membrane. Each measurement was conducted in triplicate to ensure reproducibility. [37][41].

5. Photocatalytic Test

Photocatalytic performance of the membranes was evaluated using tartrazine degradation as a model reaction. In the UV Vis spectrum of tartrazine, the absorption band at 258 nm is associated with aromatic ring transitions. In comparison, the maximum absorption at 427 nm corresponds to chromophoric groups such as N=N, C=N, and C=O that contribute to the characteristic yellow color of the dye [2][42][43].

Absorbance measurements were recorded at 1-hour intervals using two sequential stages: 1 hour in the dark, followed by 2 to 6 hours under illumination. Photocatalysis was conducted using an 8 W lamp positioned 15 cm above the sample surface. The lamp emitted white light across the visible region (approximately 400 to 700 nm), covering the absorption range of tartrazine. The irradiation intensity received by the sample was estimated to be at most 28.3 W.m^{-2} . A dark adsorption step was applied for 1 hour before irradiation to establish an adsorption-desorption equilibrium between tartrazine and the membrane surface. This step ensures that concentration changes observed during the light exposure phase primarily reflect photocatalytic degradation rather than initial adsorption. Absorbance was measured after the dark period, defined as $t = 0$ for the illumination stage, and continued to be monitored during irradiation from $t = 2$ to 6 hours to track degradation.

The absorbance data were used to calculate tartrazine degradation efficiency and reaction kinetics using a pseudo-first-order model. The apparent reaction rate constant ($k=\text{h}^{-1}$) was determined from:

$$\ln \left(\frac{C_0}{C_t} \right) = kt \quad (2)$$

where C_0 is the initial concentration, and C_t is the concentration at time t . Model reliability was evaluated based on the linear regression coefficient, with R^2 values above 0.95 indicating a good fit [44].

RESULT AND DISCUSSION

This study aims to develop a chitosan-based membrane incorporating Mn-doped ZnO at a doping level of 30%, which has been identified as an effective composition for the photocatalytic degradation of tartrazine dye. Glycerol was added to the membrane formulation as a plasticizer to improve membrane flexibility and structural homogeneity. To assess the influence of glycerol, membranes containing glycerol were directly compared with membranes prepared without glycerol. A comprehensive set of characterizations was performed to evaluate membrane morphology, physical properties, and photocatalytic performance. The results are presented systematically, beginning with macroscopic observations and followed by detailed analyses using microscopic, spectroscopic, and photocatalytic degradation tests

1. Membran Visualization

Initial observations were focused on visual descriptions of membranes to assess the differences in color, elasticity, and homogeneity between the two types of membranes. A visual description of the membrane is shown in Figure 1. Macroscopically, the chitosan-ZnO doping membrane Mn, without the addition of glycerol, exhibits a rougher surface with a color that tends to be pale yellowish to brownish. Physically, this membrane appears stiffer and brittle when folded, indicating that the absence of a plasticizer causes the interaction between components to be less

than optimal, making the membrane structure more rigid and prone to cracking.

The chitosan-ZnO-doped Mn 30% membrane, with the addition of glycerol, appears homogeneous and has a relatively flat surface. The color of the membrane tends to be cloudy white to yellowish, depending on the concentration of Mn doping, with good elasticity and not brittle when folded. This

homogeneity and flexibility indicate an effective mixing between chitosan, ZnO, Mn, and glycerol in a membrane matrix. This reinforces the role of glycerol in enhancing flexibility, improving adhesion between particles, and promoting membrane homogeneity [45].

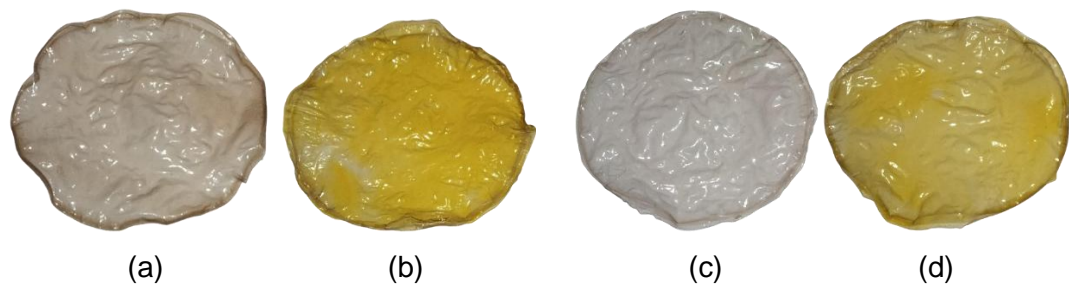


Figure 1. Chitosan-ZnO dop Mn membrane (a) without glycerol before photocatalysis (b) without glycerol after photocatalysis (c) with glycerol before photocatalysis (d) with glycerol after photocatalysis

Table 1. Membrane Adsorption Capacity to Tartrazine

Time (hours)	Treatment	Absorbance	%Degradation
1	without glycerol	0,137	49%
2		0,100	63%
3		0,080	70%
4		0,061	77%
5		0,036	87%
6		0,012	95%
1	with glycerol	0,155	42%
2		0,148	45%
3		0,136	49%
4		0,121	55%
5		0,112	58%
6		0,100	62%

Figure 1 shows visual changes in the chitosan-ZnO membrane doping Mn 30%, both with and without the addition of glycerol, before and after the photocatalysis process of

tartrazine solution. In membranes without glycerol (a and b), a significant color difference is observed. The color of the membrane after photocatalysis (b) becomes more yellowish, which indicates that the tartrazine molecule has been absorbed and degraded on the active surface of the membrane. This indicates that membranes without glycerol exhibit better photocatalytic activity and adsorption capabilities, as the active surface of ZnO-additional compounds do not obstruct Mn. In contrast, glycerol-containing membranes (c and d) did not show a marked discoloration after photocatalysis. The yellow color on the d-membrane still appears strong, indicating that the degradation of tartrazine is not occurring optimally. This condition is most likely caused

by the presence of glycerol, which forms a barrier layer on the surface of the membrane, thereby inhibiting the diffusion of tartrazine molecules and reducing the effectiveness of charge transfer in photocatalytic processes. This finding aligns with research conducted by Nhung et al. in 2023 on the Chitosan/TiO₂/Glycerol Film, which suggests that excessive glycerol can reduce the formation of reactive oxygen species (ROS) and inhibit the degradation process by interfering with the efficiency of charge transfer between chitosan and TiO₂ [34]. To support the visual data, the membrane's adsorption capacity quantitatively reflects its effectiveness.

Based on the data in Table 1, there is a significant difference in the process of tartrazine degradation between the addition of glycerol and its absence. In a system without glycerol, degradation increases

sharply over time, reaching 95% by the 6th hour, indicating that the photocatalysis process is highly effective. In contrast, in systems with the addition of glycerol, the decrease in absorbance occurs more slowly, with degradation reaching only 62% by the 6th hour. This indicates that the presence of glycerol tends to inhibit the rate of tartrazine degradation. It is indicated that glycerol acts as a competitive compound that reacts with active radicals in the photocatalytic system [33].

Although glycerol can improve the flexibility and homogeneity of the membrane [46], its presence actually decreases the photodegradation efficiency of dyestuffs. The difference in visual response between these two types of membranes reinforces the notion that surface structure and composition play a crucial role in photocatalytic effectiveness.

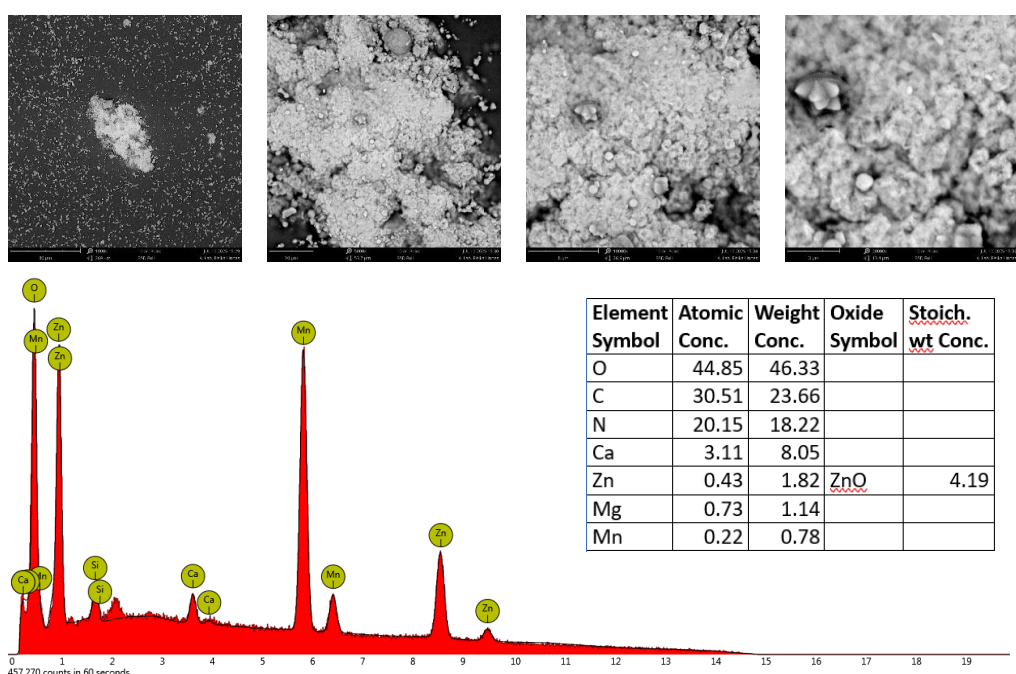


Figure 2. SEM-EDX Test Results on Membrane of Chitosan-Mn doped ZnO 30% without Glycerol

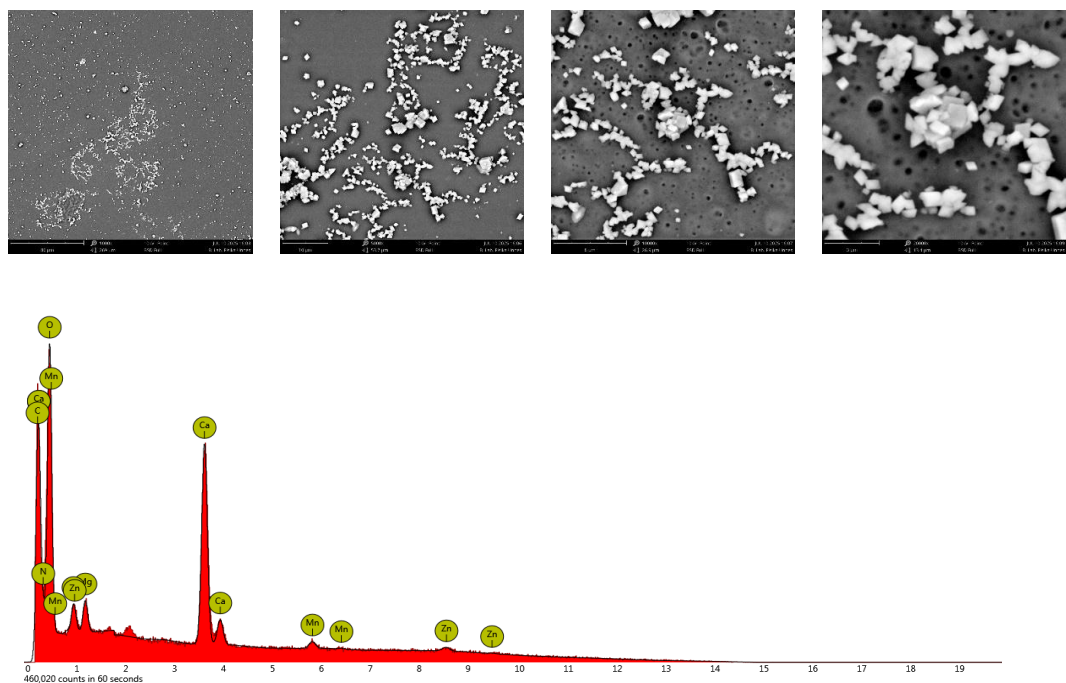


Figure 3. SEM-EDX Test Results on the Membrane of Chitosan-Mn doped ZnO 30% with Glycerol

Surface morphological analysis using Scanning Electron Microscopy (SEM) revealed that the chitosan-ZnO membrane doped with Mn, without the addition of glycerol, exhibits a rough and inhomogeneous surface structure (Figure 2). There is a fairly large agglomeration of particles, which indicates an uneven distribution of ZnO in the chitosan matrix. The absence of glycerol as a plasticizer is thought to be the main cause of the formation of brittle and non-uniform porous surfaces, because glycerol generally functions to increase the flexibility and homogeneity of materials [27][33].

The results of Energy Dispersive X-ray Spectroscopy (EDX) confirmed the presence of the main elements that make up the membrane, namely O (44.85 at%), C (30.51 at%), and N (20.15 at%), which

correspond to the basic structure of chitosan. In addition, the element Zn was detected at 0.43 at% with a weight concentration of 1.82%, indicating the presence of ZnO in the system, albeit with limited distribution. Mn as dopant was also detected in small amounts, namely 0.22 at%, indicating that doping was successfully carried out but was not optimal in terms of quantity and distribution. The stoichiometric value of ZnO formed, based on the weight concentration, reached 4.19%, indicating that ZnO has been dispersed in the matrix [47]. However, there is a need for improved mixing methods to achieve a more even distribution. The presence of small amounts of Ca and Mg elements is likely due to material residues or contamination during the synthesis process.

SEM observations indicate that the addition of glycerol has a substantial

influence on the surface morphology of the Mn-doped chitosan ZnO membrane (Figure 3). The glycerol-modified membrane exhibits a smoother and more homogeneous surface with a more uniform particle distribution compared to the membrane prepared without glycerol. Bright crystallite features attributed to ZnO and Mn-containing phases are more evenly dispersed and show less pronounced agglomeration, suggesting that glycerol contributes not only as a plasticizer but also as a dispersing and homogenizing agent within the polymer matrix.

EDX analysis further supports these observations. The glycerol-containing membrane exhibited higher detected Zn and Mn atomic fractions, with Zn increasing to 20.56 at% and Mn to 19.04 at%, which are substantially higher than those in the membrane without glycerol. The presence of oxygen (44.35%) and nitrogen (13.40%) is

consistent with contributions from metal oxide components and the functional groups of chitosan. In addition, the calculated ZnO mass fraction was 55.89%, indicating effective incorporation of ZnO into the membrane structure. Overall, glycerol promotes the improved dispersion of inorganic particles within the chitosan matrix, producing a more uniform membrane morphology that may support better performance in subsequent functional applications.

2. Membrane Physical Characterization

Physical tests were performed to determine the basic characteristics of chitosan-ZnO-based membranes doped with Mn, either with or without the addition of glycerol. The physical tests carried out include a thickness test, a tensile test, a porosity test, and a water contact angle test.

Table 2. Results of Membrane Thickness, Porosity Test, and Water Contact Angle Test Without or with Glycerol

Membrane Composition	Thickness (μm) ± SD	%porosity	Contact angle (°) ± SD
Chitosan-ZnO doping Mn 30% without glycerol	0.0035 ± 0.0001 μm	78	91,40 ± 0,11
Chitosan-ZnO doping Mn 30% with glycerol	0.0040 ± 0.0001 μm	44	99,17 ± 0,12

Table 3. Membrane Tensile Test Results without or with glycerol

Membrane	Yield Strength (N/mm ²)	Tensile Strength (N/mm ²)	Elongation (%)	Young's M (N/mm ²)
Without glycerol	14.22	21.81	18.33	397.70
With glycerol	18.12	32.07	38.29	134.05

a. Membrane Thickness Test

Observations showed that the glycerol-containing membrane tended to be thicker than the membrane prepared without glycerol. This increase in thickness is likely related to the role of glycerol as a plasticizer,

which enhances chain mobility and retains moisture, potentially promoting denser film formation during drying and resulting in a thicker membrane. Thickness values were obtained from three replicate measurements and are reported as mean values. The small

standard deviation (SD = 0.0001 μm) indicates minimal variation among replicates, suggesting high measurement consistency. A comparison of membrane thickness is presented in [Table 2](#).

b. Tensile Strength Test

Results in [Table 3](#) show that glycerol addition significantly increased tensile strength and elongation, while decreasing Young's modulus. The glycerol-modified membrane exhibited a tensile strength of 32.07 N/mm², higher than the membrane without glycerol (21.81 N/mm²). Elongation at break also increased markedly from 18.33% to 38.29%, indicating improved elasticity and ductility.

The increase in elongation supports the role of glycerol as a plasticizer that enhances membrane flexibility by reducing intermolecular interactions between polymer chains. In contrast, Young's modulus decreased substantially from 397.70 N/mm² to 134.05 N/mm², indicating reduced stiffness, which is consistent with the expected behavior of plasticized polymer systems.

Yield strength increased from 14.22 N/mm² to 18.12 N/mm², indicating that the glycerol-containing membrane can withstand higher stress before entering the plastic deformation region. Overall, the data in [Table 3](#) indicate that glycerol improves not only flexibility but also the membrane's resistance to mechanical loading before failure.

Similar trends have been reported in related work. Nhung et al. (2023) developed CTiG films (100 \times 50 mm; thickness, 0.15 \pm 0.03 mm; density, 1.141 \pm 0.12 g/cm³) and noted a relatively high tensile strength,

although specific tensile strength values were not reported [\[34\]](#).

c. Porosity Test

[Table 2](#) shows that the membrane without glycerol had a porosity of 78%, whereas the membrane containing glycerol exhibited a much lower porosity of 44%. This substantial decrease suggests that glycerol promotes the formation of a denser and more compact membrane structure. One possible explanation is that glycerol increases the mobility of polymer chains during casting and drying, allowing chitosan chains to pack more efficiently and thereby reducing the total void volume that remains as pores in the final film.

Glycerol addition also appears to alter pore morphology. The glycerol-free membrane tends to display smaller and more uniformly distributed pores that originate from inherent free volume between polymer chains. In contrast, glycerol-modified membranes may exhibit a broader pore size distribution and less uniform pore structure due to changes in chain arrangement and local microphase behavior during solvent evaporation. This structural rearrangement can reduce overall porosity even when some pores appear larger.

The decrease in porosity has significant implications for membrane performance, particularly in terms of flux and selectivity. Lower porosity generally reduces permeation rate but can increase selectivity because diffusion pathways become more restricted and controlled [\[40\]\[48\]](#). This trade off must be considered based on application needs. Membranes intended for finer separation may benefit from reduced porosity combined with improved mechanical

strength, as supported by the tensile results. In contrast, applications requiring high water flux may be hindered by excessive reduction in porosity. The porosity results in [Table 2](#) also appear to contrast with the common expectation that plasticizers increase free volume and thereby increase porosity. This discrepancy suggests that additional factors dominate pore formation in this system. Glycerol may not only act as a plasticizer but also form strong hydrogen bonding interactions with chitosan, which can suppress pore generation during casting and drying and ultimately yield a tighter membrane network [\[33\]\[34\]](#).

d. Water Contact Angle Test

[Table 2](#) shows that the membrane without glycerol had an average water contact angle of $91.40 \pm 0.11^\circ$, whereas the glycerol-containing membrane exhibited a higher contact angle of $99.17 \pm 0.12^\circ$. Because both values exceed 90° , both membranes can be classified as hydrophobic, with the glycerol-modified membrane showing lower wettability. The increase in contact angle after glycerol addition is likely associated with structural changes in the chitosan matrix that produce a denser and smoother surface, thereby limiting water penetration. Glycerol can also occupy or partially block microscopic surface pores, reduce surface free energy, and consequently enhance apparent hydrophobicity [\[41\]\[49\]](#). These wettability changes may influence tartrazine adsorption on the membrane surface and affect interfacial charge transfer during

photodegradation, which is discussed further in the photocatalytic mechanism section.

3. Photocatalytic Test

Visual monitoring of tartrazine degradation using chitosan–ZnO membranes with 30% doping, prepared with and without glycerol, was conducted as an initial step to assess photocatalytic performance qualitatively. These observations provide a direct indication of photodegradation under visible light irradiation. Changes in the color intensity of the tartrazine solution over time were recorded to obtain a preliminary overview of degradation progress and relative reaction rates prior to quantitative evaluation using UV Vis spectrophotometry. The photocatalytic test results are summarized in [Table 4](#).

During the 1-hour dark phase, the chitosan Mn-doped ZnO membrane without glycerol showed a visible decrease in the yellow intensity of the tartrazine solution. This observation suggests that tartrazine adsorption onto the membrane surface occurred before irradiation. Adsorption is an important preliminary step because it determines the number of pollutant molecules that can reach and interact with photocatalytically active sites.

In contrast, the glycerol-modified membrane showed no noticeable color change during the dark phase, suggesting weaker tartrazine adsorption. This behavior is consistent with the possibility that glycerol partially covers the available surface sites, thereby reducing the accessibility of tartrazine molecules to the catalyst interface.

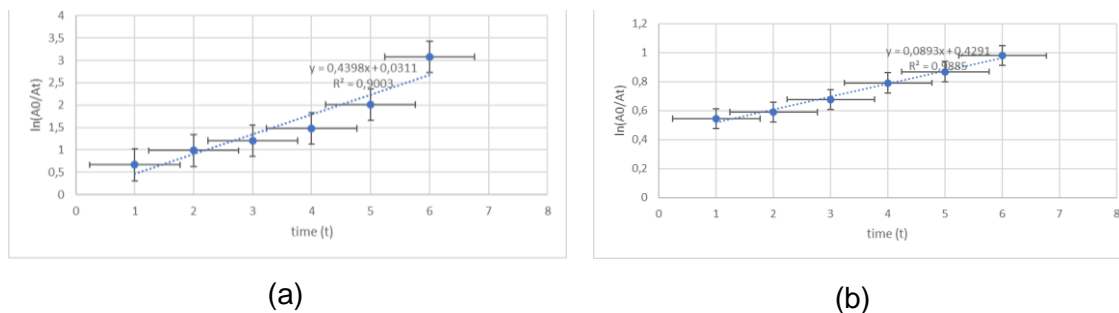


Figure 4. Kinetic graph of a pseudo-order one-order reaction for the degradation of tartrazine (a) chitosan-ZnO membrane dop Mn without glycerol, (b) chitosan membrane-ZnO dop Mn with glycerol

Table 4. Chitosan-ZnO dop Mn membrane Photocatalytic Test Results with or without glycerol

membrane	Treatment & Timing					
	Dark 1 hour	Bright 2 hour	3 hour	4 hour	5 hour	6 hour
Without glycerol						
With glycerol						

Clear differences were also observed once irradiation started (2nd to 6th hour). The membrane without glycerol produced progressive discoloration, with the characteristic yellow color fading substantially and becoming nearly colorless by the 6th hour, indicating more effective photodegradation. Under visible light, excitation of the Mn-doped ZnO phase promotes electron-hole pair generation, which can lead to the formation of reactive species such as hydroxyl radicals and superoxide radicals that break down the tartrazine structure [50][51].

The glycerol-containing membrane showed a significantly slighter decrease in

color intensity, with the yellow coloration remaining relatively strong at the end of the irradiation period. This result suggests less efficient generation of reactive species. Glycerol can form hydrogen bonds with functional groups in the membrane and interact with surface hydroxyl sites, potentially creating a partial blocking layer around Mn-doped ZnO that limits tartrazine diffusion and interferes with interfacial charge transfer required for radical formation [52]. The reduced porosity and higher contact angle observed for glycerol-modified membranes may further limit effective contact between the dye solution and the

photocatalyst surface, contributing to slower degradation.

[Figure 4](#) presents the pseudo-first-order kinetic plots for tartrazine degradation using (a) the Mn-doped ZnO chitosan membrane without glycerol and (b) the corresponding membrane containing glycerol. Photocatalytic tests indicate that tartrazine degradation in both systems follows pseudo-first-order kinetics, as reflected by the relatively high coefficients of determination (R^2). The membrane without glycerol exhibits an R^2 value of 0.9003, while the glycerol-modified membrane shows an R^2 value of 0.9885, indicating a good linear fit in both cases.

[Figure 4](#) also highlights a clear difference in the apparent reaction rate constant (k). The membrane without glycerol exhibits a higher k value of 0.4398 h^{-1} , whereas the membrane with glycerol shows a substantially lower k value of 0.0893 h^{-1} . A higher k value indicates faster tartrazine degradation, confirming that the glycerol-free membrane achieved superior photocatalytic activity under the tested conditions [\[53\]](#).

This performance gap can be attributed to differences in the physicochemical properties of the membranes. Glycerol improves flexibility and mechanical strength, yet it can reduce porosity and increase the water contact angle, which may limit tartrazine adsorption and hinder mass transfer within the membrane. Glycerol can also partially mask ZnO Mn active sites through hydrogen bonding and polar interactions, which can reduce interfacial charge transfer efficiency and suppress the formation of reactive

species responsible for tartrazine degradation [\[17\]](#)[\[18\]](#). The combined effect is a lower availability of radicals that drive the oxidation process.

Additional factors may contribute, including light attenuation and surface shielding. Changes in morphology and refractive index associated with glycerol can increase light scattering or reflection, reducing the photon flux reaching ZnO Mn sites. A glycerol-rich layer surrounding particles may also act as a diffusion barrier, thereby decreasing tartrazine's access to active sites. Together, these effects can reduce photocatalytic efficiency, leading to the lower rate constant observed in [Figure 4](#).

Overall, the results indicate that although glycerol enhances mechanical properties, the glycerol-free formulation provides better photocatalytic performance for tartrazine degradation. Optimization of glycerol content or additional surface and structural modifications may be required to balance mechanical integrity and photocatalytic activity.

4. Charge Transfer Mechanism

Understanding tartrazine photodegradation on Mn-doped ZnO membranes immobilized in a chitosan matrix requires first examining the charge transfer processes that govern photocatalytic activity. [Figure 5](#) summarizes the proposed charge transfer mechanisms for the membranes prepared without glycerol and with glycerol modification. The process of tartrazine photodegradation on the Mn-doped ZnO-Chitosan membrane involves a charge transfer mechanism initiated by the excitation of electrons from the valence band to the ZnO

conduction band due to exposure to visible light. This event produces a pair of electrons (e^-) and a hole (h^+) [54], which then play a role in the redox reaction to produce active radicals. The Mn^{2+} ions doped into the ZnO structure act as electron traps, thereby lowering the recombination rate of e^-/h^+ and

extending the life of the pair. The hole (h^+) left behind will oxidize the water molecules or OH^- ions into hydroxyl radicals ($\cdot OH$), while electrons will reduce O_2 to superoxide radicals ($\cdot O_2^-$). These two types of radicals play a major role in the degradation of the molecular structure of tartrazine.

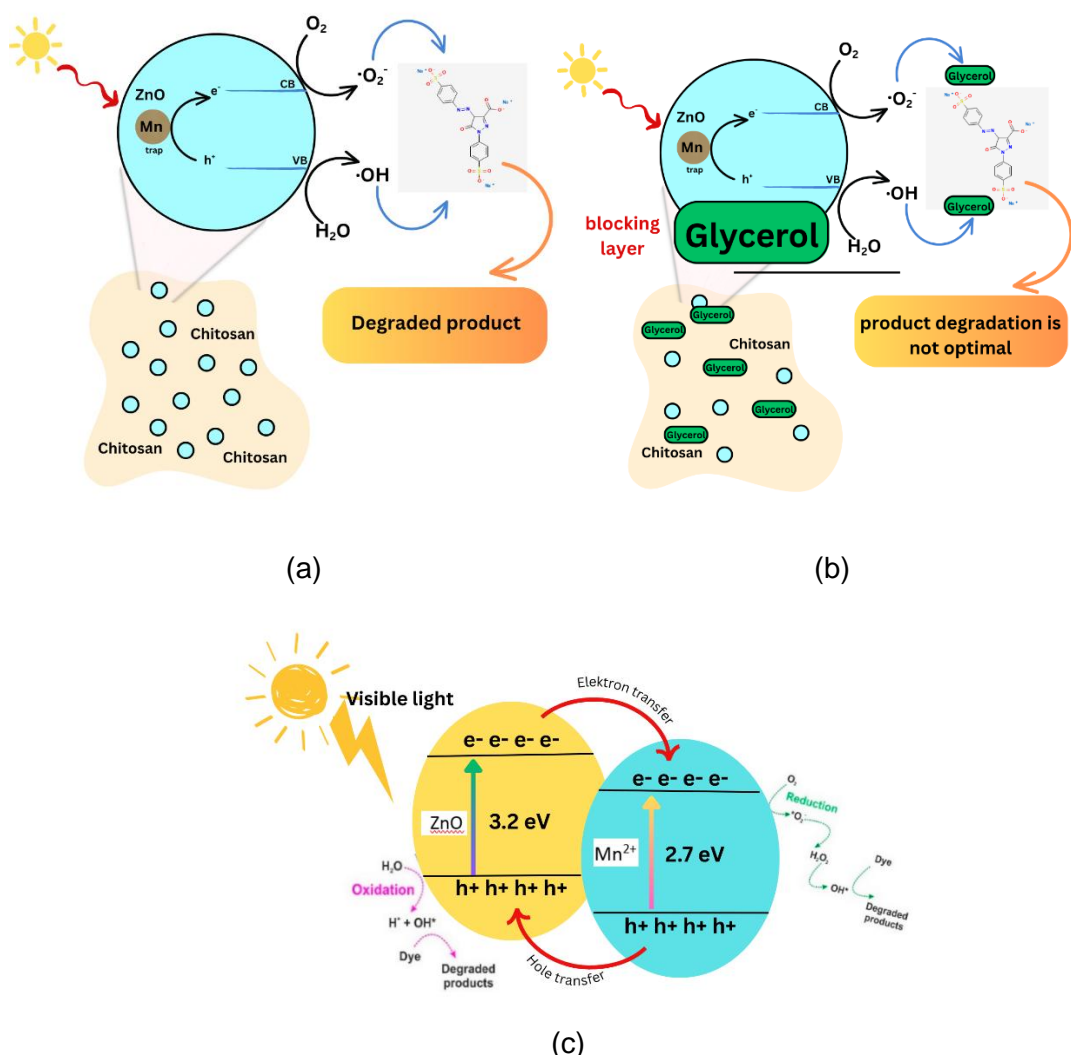


Figure 5. The mechanism of charge transfer on the membrane combined (a) without glycerol, (b) with glycerol, (c) Band Diagram Energy Levels and Mn^{2+} Trapping States.

In membranes without glycerol, this charge transfer process takes place more efficiently because there is no barrier on the active surface, so that radical formation and interaction with tartrazine molecules can

occur optimally. In contrast, the addition of glycerol to the membrane matrix is known to improve flexibility and mechanical stability, but also hurt photocatalytic activity. [1], [27].

Glycerol, being polyhydroxy, can interact strongly with the membrane surface and active sites of ZnO–Mn through hydrogen bonds, thereby forming a *blocking layer*. This coating can limit the diffusion of O₂, H₂O, or tartrazine to the active surface as well as inhibit the transfer of the charge necessary for radical formation. Therefore, although structurally stronger, membranes with glycerol exhibit decreased effectiveness in the photodegradation process due to limited surface reactivity resulting from blocking sites and changes in surface properties that render them more hydrophobic.

CONCLUSION

This study successfully developed and compared the photocatalytic performance of chitosan-based Mn-doped ZnO membranes prepared with and without glycerol for the degradation of tartrazine under visible light irradiation. Characterization results indicate that glycerol significantly enhances the physical properties of the membrane, including increased thickness, flexibility, tensile strength, and elasticity. These findings suggest that glycerol functions effectively as a plasticizer, enhancing membrane homogeneity and mechanical stability.

However, the photocatalytic performance was higher for the glycerol-free membrane. SEM-EDX observations suggest that the membrane without glycerol has a more open surface structure and more accessible ZnO–Mn particles, which supports better contact between the photocatalyst and the reaction medium. This interpretation is consistent with photodegradation results, where the glycerol-

free membrane achieved a higher apparent rate constant ($k = 0.4398 \text{ h}^{-1}$) compared with the glycerol-containing membrane ($k = 0.0893 \text{ h}^{-1}$). Both systems follow pseudo-first-order kinetics, yet the overall degradation efficiency is clearly higher in the absence of glycerol.

Charge transfer analysis indicates that visible light irradiation promotes electron excitation from the valence band to the conduction band of ZnO, generating electron-hole pairs (e and h^+) that drive the formation of hydroxyl and superoxide radicals ($\cdot\text{OH}$ and $\cdot\text{O}_2^-$). Mn²⁺ acts as an electron trap that suppresses recombination, prolongs charge carrier lifetime, and promotes radical production. In the glycerol-free membrane, charge transfer and interfacial reactions proceed more effectively because active sites remain readily accessible. In contrast, glycerol can interact with the membrane and ZnO–Mn surface through hydrogen bonding, forming a partial blocking layer that limits the diffusion of O₂, H₂O, and tartrazine to active sites and inhibits interfacial charge transfer, leading to reduced radical generation and lower degradation rates.

Overall, glycerol improves mechanical performance but can reduce photocatalytic efficiency when present at excessive levels. Optimizing glycerol content is therefore essential to balance mechanical stability and catalytic activity. Based on the trends observed in this study, glycerol content should be maintained at no more than 1 mL per 100 mL of membrane casting solution to preserve mechanical benefits without substantially compromising tartrazine degradation performance.

ACKNOWLEDGEMENT

The author would like to thank the UNDIP Chemistry Laboratory and the UNIMUS Chemistry Laboratory for the support of facilities and technical assistance provided during this research process. A heartfelt thank you is also extended to the supervisor for the guidance, direction, and motivation that were very meaningful throughout every stage of the research implementation, culminating in the preparation of this article.

REFERENCES

[1] D. A. Widyasari and K. Khasanah, "Analisis Tartrazin dalam Minuman Kemasan di Pasar Bandar, Batang secara Spektrofotometri UV-Vis," *J. Pharm.*, vol. 1, no. 1, pp. 9–20, 2023, doi: [10.30989/jop.v1i1.918](https://doi.org/10.30989/jop.v1i1.918).

[2] DS Rejeki, O Pramianti, SS Pramesti, and Muti Aryanti, "Analisis Kadar Zat Warna Tartrazin pada Makanan dan Minuman dengan Metode Spektrofotometri UV-Vis," *J. Med. Nusant.*, vol. 2, no. 4, pp. 01–13, 2024, doi: [10.59680/medika.v2i4.1429](https://doi.org/10.59680/medika.v2i4.1429).

[3] D. H. Micheletti *et al.*, "A review of adsorbents for removal of yellow tartrazine dye from water and wastewater," *Bioresour. Technol. Reports*, vol. 24, no. August, 2023, doi: [10.1016/j.biteb.2023.101598](https://doi.org/10.1016/j.biteb.2023.101598).

[4] H. Alkhaldi *et al.*, "RSC Advances Sustainable polymeric adsorbents for adsorption- based water remediation and pathogen," *RSC Adv.*, vol. 14, pp. 33143–33190, 2024, doi: [10.1039/D4RA05269B](https://doi.org/10.1039/D4RA05269B).

[5] R. Al-tohamy *et al.*, "Ecotoxicology and Environmental Safety A critical review on the treatment of dye-containing wastewater: Ecotoxicological and health concerns of textile dyes and possible remediation approaches for environmental safety," *Ecotoxicol. Environ. Saf.*, vol. 231, p. 113160, 2022, doi: [10.1016/j.ecoenv.2021.113160](https://doi.org/10.1016/j.ecoenv.2021.113160).

[6] P. Amchova, F. Siska, and J. Ruda-Kucerova, "Safety of tartrazine in the food industry and potential protective factors," *Heliyon*, vol. 10, no. 18, p. e38111, 2024, doi: [10.1016/j.heliyon.2024.e38111](https://doi.org/10.1016/j.heliyon.2024.e38111).

[7] K. Sivaranjani, S. Sivakumar, and J. Dharmaraja, "Enhancement Photocatalytic Activity of Mn Doped Cds/Zno Nanocomposites for the Degradation of Methylene Blue Under Solar Light Irradiation," *Adv. Mater. Sci.*, vol. 22, no. 2, pp. 28–48, 2022, doi: [10.2478/adms-2022-0006](https://doi.org/10.2478/adms-2022-0006).

[8] G. K. Weldegebrial, "Synthesis method, antibacterial and photocatalytic activity of ZnO nanoparticles for azo dyes in wastewater treatment: A review," *Inorg. Chem. Commun.*, vol. 120, no. June, p. 108140, 2020, doi: [10.1016/j.inoche.2020.108140](https://doi.org/10.1016/j.inoche.2020.108140).

[9] I. M. Tsani, "Review Nanopartikel ZnO: Metode Sintesis Nanopartikel dan Aplikasi dalam Dunia Kesehatan," 2021.

[10] R. T. Hussain, M. S. Hossain, and J. H. Shariffuddin, "Green synthesis and photocatalytic insights: A review of zinc oxide nanoparticles in wastewater treatment," *Mater. Today Sustain.*, vol. 26, no. January, p. 100764, 2024, doi: [10.1016/j.mtsust.2024.100764](https://doi.org/10.1016/j.mtsust.2024.100764).

[11] N. B. Kudaer, E. Yousif, M. H. Risan, and M. Khadom, "Preparation of ZnO Nanoparticles by the Chemical Precipitation Method," *J. Serambi Eng.*, vol. 7, no. 2, pp. 3129–3134, 2022,

[12] P. Kadam, K. Gadave, S. Jadkar, V. Kadam, and C. Jagtap, "C: ZnO Composites for Improving Catalytic Activity of ZnO," *ES Energy Environ.*, vol. 21, pp. 1–11, 2023, doi: [10.30919/ese946](https://doi.org/10.30919/ese946).

[13] M. A. Abu-Dalo, S. A. Al-Rosan, and B. A. Albiss, "Photocatalytic degradation of methylene blue using polymeric membranes based on cellulose acetate impregnated with ZnO nanostructures," *Polymers (Basel.)*, vol. 13, no. 19, 2021, doi: [10.3390/polym13193451](https://doi.org/10.3390/polym13193451).

[14] Y. Chi *et al.*, "Evaluation of practical application potential of a photocatalyst: Ultimate apparent photocatalytic activity," *Chemosphere*, vol. 285, p. 131323, 2021, doi: [10.1016/j.chemosphere.2021.131323](https://doi.org/10.1016/j.chemosphere.2021.131323).

[15] V. Kumaravel *et al.*, "Antimicrobial TiO₂ nanocomposite coatings for surfaces, dental and orthopaedic implants," *Chem. Eng. J.*, vol. 416, no. December 2020, p. 129071, 2021, doi: [10.1016/j.cej.2021.129071](https://doi.org/10.1016/j.cej.2021.129071).

[16] M. H. Aleinawi, A. U. Ammar, M. Buldu-Akturk, N. S. Turhan, S. Nadupalli, and E. Erdem, "Spectroscopic Probing Of Mn-Doped ZnO Nanowires Synthesized via a Microwave-Assisted Route," *J. Phys. Chem. C*, vol. 126, no. 8, pp. 4229–4240, 2022, doi: [10.1021/acs.jpcc.2c00009](https://doi.org/10.1021/acs.jpcc.2c00009).

[17] R. Akram, A. Fatima, Z. M. Almohaimeed, Z. Farooq, K. W. Qadir, and Q. Zafar, "Photocatalytic Degradation of Methyl Green Dye Mediated by Pure and Mn-Doped Zinc Oxide Nanoparticles under Solar Light Irradiation," *Adsorpt. Sci. Technol.*, pp. 1–15, 2023, doi: [10.1155/2023/5069872](https://doi.org/10.1155/2023/5069872).

[18] M. Ishfaq *et al.*, "The in situ synthesis of sunlight-driven Chitosan/MnO₂@MOF-801 nanocomposites for photocatalytic reduction of Rhodamine-B," *J. Mol. Struct.*, vol. 1301, no. November 2023, p. 137384, 2024, doi: [10.1016/j.molstruc.2023.137384](https://doi.org/10.1016/j.molstruc.2023.137384).

[19] P. Sen *et al.*, "Advancements in Doping Strategies for Enhanced Photocatalysts and Adsorbents in Environmental Remediation," *Technologies*, vol. 11, no. 5, pp. 1–31, 2023, doi: [10.3390/technologies11050144](https://doi.org/10.3390/technologies11050144).

[20] S. Sethi, Medha, and S. Thakur, "Synthesis and characterization of nanocomposite chitosan-gelatin hydrogel loaded with ZnO and its application in photocatalytic dye degradation," *Mater. Today Proc.*, vol. 78, pp. 815–824, 2023, doi: [10.1016/j.matpr.2022.11.277](https://doi.org/10.1016/j.matpr.2022.11.277).

[21] J. Kerwald, C. F. de Moura Junior, E. D. Freitas, J. de D. P. de Moraes Segundo, R. S. Vieira, and M. M. Beppu, "Cellulose-based electrospun nanofibers: a review," vol. 29, no. 1. 2022. doi: [10.1007/s10570-021-04303-w](https://doi.org/10.1007/s10570-021-04303-w).

[22] S. Acharya, S. Liyanage, N. Abidi, P. Parajuli, S. S. Rumi, and J. L. Shamshina, "Utilization of cellulose to its full potential: A review on cellulose dissolution, regeneration, and applications," *Polymers (Basel.)*, vol. 13, no. 24, 2021, doi: [10.3390/polym13244344](https://doi.org/10.3390/polym13244344).

[23] S. D. and P. D. P. Galina Satchanska, "Natural and Synthetic Polymers for Biomedical and Environmental Applications Galina," *Polymers (Basel.)*, vol. 16, no. 1159, pp. 591–641, 2024, doi: [10.3390/polym16081159](https://doi.org/10.3390/polym16081159) Academic.

[24] S. A. Elsayed, I. E. T. El-Sayed, and M. A. Tony, "Impregnated chitin biopolymer with magnetic nanoparticles to immobilize dye from aqueous media as a simple, rapid and efficient composite photocatalyst," *Appl. Water Sci.*, vol. 12, no. 11, pp. 1–16, 2022, doi: [10.1007/s13201-022-01776-3](https://doi.org/10.1007/s13201-022-01776-3).

[25] F. R. Pramastuti, E. Supriyantini, R. Pramesti, S. Sedjati, and A. Ridlo, "Kitosan sebagai Biodsorben Logam Besi (Fe) pada Jaringan Lunak Kerang Hijau (Perna viridis)," *Bul. Oseanografi Mar.*, vol. 13, no. 1, pp. 63–69, 2024, doi: [10.14710/buloma.v13i1.41095](https://doi.org/10.14710/buloma.v13i1.41095).

[26] V. Virrisya and A. Astuti,

[26] "Karakterisasi Sifat Optik Nanopartikel ZnO didoping Mn Menggunakan Metode Sol-Gel," *J. Fis. Unand*, vol. 8, no. 4, pp. 308–314, 2019, doi: [10.25077/jfu.8.4.308-314.2019](https://doi.org/10.25077/jfu.8.4.308-314.2019).

[27] S. R. Cengristitama, "Pengaruh Penambahan Plasticizer Gliserol Dan Kitosan Terhadap Karakteristik Plastik Biodegradable Berbahan Dasar Pati Sukun," *TEDC*, vol. 16, no. 2, pp. 102–108, 2022.

[28] B. R. Widiatmono, A. A. Sulianto, and C. Debora, "Biodegradabilitas Bioplastik Berbahan Dasar Limbah Cair Tahu dengan Penguat Kitosan dan Plasticizer Gliserol," *J. Sumberd. Alam dan Lingkung.*, vol. 8, no. 1, pp. 21–27, 2021, doi: [10.21776/ub.jsal.2021.008.01.3](https://doi.org/10.21776/ub.jsal.2021.008.01.3).

[29] R. D Nyamiati, D. Timotius, S. S. Rahmawati, C. Carissavilla, and N. Amalia, "Pengaruh Kinerja Membran Kitosan-TiO₂ Terhadap Degradasi Limbah Batik dengan Sistem Hybrid Fotokatalitik Effect of Chitosan-TiO₂ Membrane Performance for the Degradation of Batik Waste with a Photocatalytic Hybrid System," *J. Ilm. Tek. Kim.*, vol. 21, no. 1, pp. 2460–8203, 2024, doi: [10.31315/e.v21i1.10734](https://doi.org/10.31315/e.v21i1.10734).

[30] J. Garcia *et al.*, "Chitosan-based glycerol-plasticized membranes: bactericidal and fibroblast cellular growth properties," *Polym. Bull.*, vol. 78, no. 0123456789, pp. 4297–4312, 2020, doi: [10.1007/s00289-020-03310-4](https://doi.org/10.1007/s00289-020-03310-4).

[31] Q. Duan, Y. Chen, L. Yu, and F. Xie, "Chitosan–Gelatin Films: Plasticizers/Nanofillers Affect Chain Interactions and Material Properties in Different Ways," *Polymers (Basel)*, vol. 14, no. 18, pp. 1–17, 2022, doi: [10.3390/polym14183797](https://doi.org/10.3390/polym14183797).

[32] D. R. Smith, A. P. Escobar, M. N. Andris, B. M. Boardman, and G. M. Peters, "Understanding the Molecular-Level Interactions of Glucosamine-Glycerol Assemblies: A Model System for Chitosan Plasticization," *ACS Omega*, vol. 6, no. 39, pp. 25227–25234, 2021, doi: [10.1021/acsomega.1c03016](https://doi.org/10.1021/acsomega.1c03016).

[33] N. T. T. Hoang, A. T. K. Tran, T. A. Le, and D. D. Nguyen, "Enhancing efficiency and photocatalytic activity of TiO₂-SiO₂ by combination of glycerol for MO degradation in continuous reactor under solar irradiation," *J. Environ. Chem. Eng.*, vol. 9, no. 5, p. 105789, 2021, doi: [10.1016/j.jece.2021.105789](https://doi.org/10.1016/j.jece.2021.105789).

[34] N. T. T. Hoang and D. D. Nguyen, "Improving the Degradation Kinetics of Industrial Dyes with Chitosan/TiO₂/Glycerol Films for the Sustainable Recovery of Chitosan from Waste Streams," *Sustain.*, vol. 15, no. 8, 2023, doi: [10.3390/su15086979](https://doi.org/10.3390/su15086979).

[35] A. T.-K. T. Nhungh Thi-Tuyet Hoang and Ho, "Enhanced degradation of dyes in secondary textile wastewater: Continuous-flow photoreactors using TiO₂/chitosan/glycerol under UVA irradiation," *Water Sci. Eng.*, vol. 18, no. 2, p. 107386, 2025, doi: [10.1016/j.wse.2025.08.001](https://doi.org/10.1016/j.wse.2025.08.001).

[36] N. T. T. Hoang, A. T. K. Tran, M. H. Hoang, T. T. H. Nguyen, and X. T. Bui, "Synergistic effect of TiO₂/chitosan/glycerol photocatalyst on color and COD removal from a dyeing and textile secondary effluent," *Environ. Technol. Innov.*, vol. 21, p. 101255, 2021, doi: [10.1016/j.eti.2020.101255](https://doi.org/10.1016/j.eti.2020.101255).

[37] R. A. L. Tauhid Nur Ikhsan, Khabibi, "Sintesis Membran Kitosan Tertaut Silang Tripolifosfat dengan Paduan Polivinil Alkohol untuk Permeasi Kreatinin Tauhid," *Greensph. J. Environ. Chem.*, vol. 4, no. 1, pp. 25–31, 2024, doi: [10.14710/gjec.2024.21044](https://doi.org/10.14710/gjec.2024.21044).

[38] C. G. F. Retno Ariadi Lusiana, Ahmad Suseno, Khabibi, "Pengaruh Tripolifosfat sebagai Agen Taut Silang pada Membran Kitosan Terhadap Karakter Fisikokimia dan Kemampuan Permeasi," *Greensph. J. Environ. Chem.*, vol. 1, no. 1, pp. 19–

24, 2021, doi: [10.14710/gjec.2021.10898](https://doi.org/10.14710/gjec.2021.10898).

[39] A. A. S. Alahl, H. A. Ezzeldin, A. A. Al-Kahtani, S. Pandey, and Y. H. Kotp, "Synthesis of a Novel Photocatalyst Based on Silicotitanate Nanoparticles for the Removal of Some Organic Matter from Polluted Water," *Catalysts*, vol. 13, no. 6, 2023, doi: [10.3390/catal13060981](https://doi.org/10.3390/catal13060981).

[40] S. M. Sari, A. L. R., Sulaiman, D., Ulva, "Karakterisasi Membran Kitosan Kulit Udang-PVA dengan Variasi Karbon Aktif sebagai Filter Air," *J. Literasi Pendidik. Fis.*, vol. 5, no. 2, pp. 198–210, 2024, doi: [10.30872/jlpf.v5i2.4400](https://doi.org/10.30872/jlpf.v5i2.4400).

[41] K. R. Winandri, A. P. Anjuda, and S. S. Santi, "Pengaruh Ketebalan Membran Terhadap Sifat-Sifat Membran (Contact Angle , Porositas dan Selektivitas)," *J. Serambi Eng.*, vol. X, no. 1, pp. 11491–11498, 2025, [

The Effect of Heat Treatment on the Sol – Gel Preparation of TiO₂ / ZnO Catalysts and Their Testing in the Photodegradation of Tartrazine," *Appl. Sci.*, vol. 14, no. 9872, pp. 1–13, 2024, doi: [/10.3390/app14219872](https://doi.org/10.3390/app14219872).

[43] E. Renouvelables, B. Ismail, and W. Tipaza, "Preparation And Characterization Of TiO₂-Chitosan Composite Films And Application For Tartrazine Dye Degradation," *Cellul. Chem. Technol.*, vol. 9–10, no. 1101–1107, pp. 6–12, 2022. doi: [0.35812/cellulosechemtechnol.2022.56.98](https://doi.org/0.35812/cellulosechemtechnol.2022.56.98)

[44] A. M. P. Omkar V. Vani, "Solar - Powered Remediation of Carcinogenic Chromium (VI) and Methylene Blue Using Ferromagnetic Ni₁₂P₅ and Porous Ni₁₂P₅-rGO Nanostructures," *MetalMat*, pp. 1–11, 2025, doi: [10.1002/metm.70010](https://doi.org/10.1002/metm.70010).

[45] A. Hachity-ortega *et al.*, "E ect of glycerol on properties of chitosan / chlorhexidine membranes and antibacterial activity against *Streptococcus mutans*," *microbiology*,

[46] F. Z. Kocak, M. Yar, and I. U. Rehman, "Glycerol-Functionalized Chitosan-Based Injectable Hydrogels with Improved Mechanical and Proangiogenic Performance," *Int. J. Mol. Sci. Artic.*, vol. 23, no. 5370, pp. 1–17, 2022, doi: [10.3390/ijms23105370](https://doi.org/10.3390/ijms23105370)

[47] S. Raha, "ZnO nanostructured materials and their potential applications: progress, challenges and perspectives," *Nanoscale Adv.*, vol. 4, no. 1868, pp. 1868–1925, 2022, doi: [10.1039/d1na00880c](https://doi.org/10.1039/d1na00880c).

[48] U. Fathanah, M. Rahmah, S. Muchtar, M. Yusuf, and C. Meurah, "Sintesis , Karakterisasi dan Kinerja Membran Hidrofobik Menggunakan Polyvinyl Pyrrolidone (PVP) sebagai Aditif," *ALCHEMY J. Penelit. Kim.*, vol. 17, no. 2, pp. 140–150, 2021, doi: [10.20961/alchemy.17.2.48435.140-150](https://doi.org/10.20961/alchemy.17.2.48435.140-150).

[49] A. A. Refaee *et al.*, "Cellulosic fabrics modified with polyphosphonium chitosan hydrazone-TiO₂-Ag nanobiocomposites for multifunctional applications," *Int. J. Biol. Macromol.*, vol. 220, no. July, pp. 482–492, 2022, doi: [10.1016/j.ijbiomac.2022.08.104](https://doi.org/10.1016/j.ijbiomac.2022.08.104).

[50] B. Abebe, "A critical mini-review on doping and heterojunction formation in ZnO-based catalysts," *RSC Adv.*, vol. 14, no. 17338, pp. 17338–17349, 2024, doi: [10.1039/d4ra02568g](https://doi.org/10.1039/d4ra02568g).

[51] N. F. R. Tang, D. Tahir, and H. Heryanto, "Sintesis Komposit ZnO/Ca₃(PO₄)₂ menggunakan metode Sol-gel sebagai Material Fotokatalis Limbah Cair Industri (Metilen Biru)," *J. Fis. Flux J. Ilm. Fis. FMIPA Univ. Lambung Mangkurat*, vol. 19, no. 1, p. 31, 2022, doi: [10.20527/flux.v19i1.11824](https://doi.org/10.20527/flux.v19i1.11824).

[52] K. T. Rashid, H. M. Alayan, A. E. Mahdi, M. N. Al-baiati, and H. S. Majdi, "Novel Water-Soluble Poly(terephthalic-co-glycerol-g-fumaric acid) Copolymer

Nanoparticles Harnessed as Pore Formers for Polyethersulfone Membrane Modification ;," *water*, vol. 14, no. 1507, pp. 1–19, 2022, doi: [10.3390/w14091507](https://doi.org/10.3390/w14091507).

[53] L. V. Quang and A. Vu, "Preparation of Au / ZnO / Fe 3 O 4 Composite for Degradation of Tartrazine under Visible Light," *vol. 18, no. 1, pp. 71–84, 2023, doi: 10.9767/bcrec.17061.*

[54] I. Aadnan, O. Zegaoui, A. El Mragui, I. Daou, H. Moussout, and J. C. G. Esteves da Silva, "Structural, Optical and Photocatalytic Properties of Mn Doped ZnO Nanoparticles Used as Photocatalysts for Azo-Dye Degradation under Visible Light," *Catalysts*, vol. 12, no. 11, 2022, doi: [10.3390/catal12111382](https://doi.org/10.3390/catal12111382).